ACS APPLIED MATERIALS & INTERFACES

Research Article

www.acsami.org

Novel Spiral-Like Electrode Structure Design for Realization of Two Modes of Energy Harvesting

Lin Chen,[†] Hengyu Guo,[†] Xiaona Xia,[†] Guanlin Liu,[†] Haofei Shi,[‡] Mingjun Wang,[†] Yi Xi,[†] and Chenguo Hu*[,†]

[†]Department of Applied Physics, Chongqing University, Chongqing 400044, P. R. China

[‡]Chongqing Engineering Research Center of Graphene Film Manufacturing, Chongqing 401329, P. R. China

Supporting Information

ABSTRACT: A planar spiral-like electrodes (PSE) based triboelectric generator has been designed for harvesting rotary mechanical energy to translate into electricity. The performance of the PSE-triboelectric generator with different cycles of spiral-like electrode strip at different rotating speeds is investigated, which demonstrates the open-circuit voltage and short-circuit current of 470 V and 9.0 μA at rotating speed of 500 r/min with three cycles. In addition, a novel coaxially integrated multilayered PSE-triboelectric generator is built, which can enhance the output of the power effectively. The short-circuit current, the open-circuit voltage, and output power reach to 41.55 μA, 500 V, and 11.73 mW, respectively, at rotating speed of 700 r/min. The output power of the multilayered PSE-triboelectric generator can drive 200 LEDs connected in antiparallel and charge a 110 μF commercial capacitor to 6 V in 23 s. Besides, due to the spiral-like electrode structure, the PSE-generator can work simultaneously in the modes of triboelectricity and electromagnetic induced electricity by sticking a small magnet on the rotating disk. The electromagnetic induced output power reaches to 21 μW at a loading resistance of 2 Ω at a rotating rate of 200 r/min. The spiral-like electrode structure not only broadens the electrode structure design but also adds a new function to the electrode.

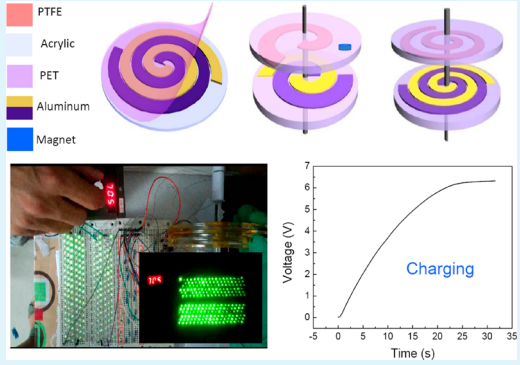

KEYWORDS: *planar spiral-like electrode, triboelectric nanogenerator, electromagnetic generator, multilayered, rotary mechanical energy*

1. INTRODUCTION

Due to worldwide ever-increasing energy consumption and environmental pollution, green energy and sustainable development have aroused public concern.[1,2] Harvesting energy from our surroundings is a good choice to meet the energy needs without causing unexpected environmental issues.[3−7] Among various energy sources, mechanical energy is universally available and environmental friendly. Nanogenerators as invented in 2006 can be a very effective and applicable technology[8−10] and it can convert environment mechanical energy into electricity based on piezoelectric effect,[11,12] triboelectric effect,[13−16] and polyelectric effect,[17−19] respectively. The triboelectric nanogenerator (TENG) has been regarded as an effective method for harvesting all kinds of mechanical energy, such as wind power,[20] wave energy,[21] and walking energy[22] due to its high efficiency, simple fabrication, low cost, and good flexibility. It is well-known that the electromagnetic generator (EMG) based on the electromagnetic induction is one of the most important means for power generation.[23] Therefore, the hybrid of TENG and EMG can improve the conversion efficiency of nanogenerators.[24−28]

There are two basic working modes of TENG with distinct characteristics, contact mode and sliding mode. Compared with the contact mode based on repeated vertical contact and separation between two materials with different triboelectric polarities, sliding mode depending on the relative displacement between two contact surfaces of different triboelectric polarities is more suitable for electrode structure improvement to enhance conversion efficiency and realize multifunction.[29,30] Very recently, the checker-like interdigital electrodes based TENG has been designed which has advantage of harvesting plane sliding energy in all directions.[31] The novel cylindric spiral interdigital-electrode design endows the generator with dual-function for harvesting rotational energy and translational motion energy, and meanwhile, have dual-function as a sensor for detecting rotating speed and momentum of moving object.[32] Therefore, patterned electrodes are important for the realization of multifunction and electronic device integration.

Here, novel planar spiral-like electrodes (PSE) generator is designed and fabricated to harvest rotary mechanical energy. The short-circuit current (I_{sc}) and the open-circuit voltage

Received: April 27, 2015
Accepted: July 7, 2015
Published: July 7, 2015

DOI: 10.1021/acsami.5b03613
ACS Appl. Mater. Interfaces 2015, 7, 16450−16457

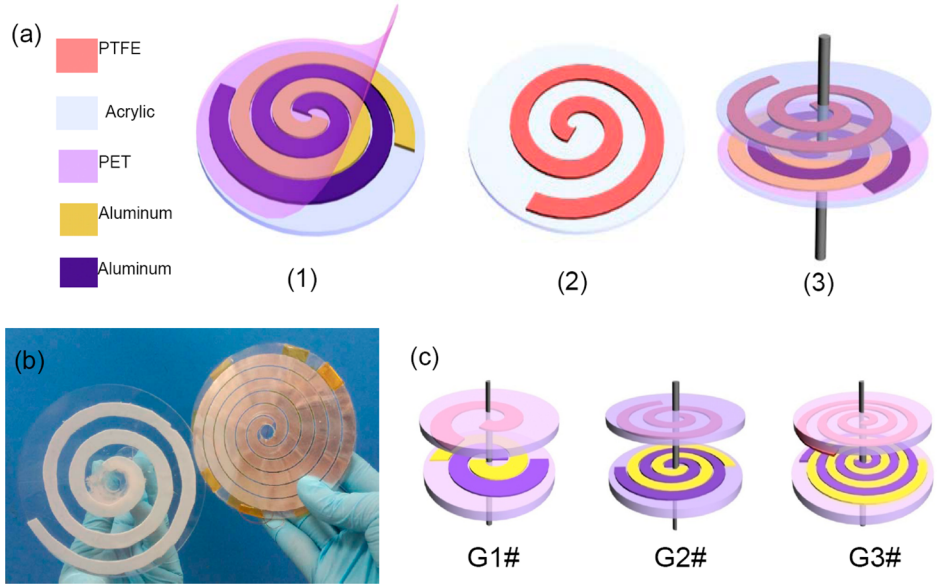

Figure 1. Structure of the PSE-triboelectric nanogenerator. (a) The stationary part of aluminum electrodes with PET film (1). The rotational part of a PTFE tribo-charged layer (2). The whole structure of the assemble PSE-triboelectric nanogenerator (3). (b) A digital photograph of the two parts of PSE-triboelectric nanogenerator. (c) The PSE-triboelectric nanogenerators with one (G1#), two (G2#), and three (G2#) of electrode cycles.

(V_{oc}) of the PSE-triboelectric generator with three cycles of the spiral-like electrode strips are 9.0 μA and 470 V, respectively, at the rotating speed of 500 r/min, and the maximum power is 3.46 mW at rotating speed of 700 r/min. Furthermore, in order to efficiently utilize the input rotary energy, multilayered PSEs and PTFE strips are integrated on the disks, which are driven by coaxially transmission rotation motion. The short-circuit current of the multilayered integrated PSE-triboelectric generator tremendously increases to 41.55 μA for the six-layered PSE-triboelectric generator while the open-circuit voltage is maintained around 500 V at rotating speed of 700 r/min. The maximum power of the multilayered PSE-triboelectric generator is 11.73 mW, which is used as a direct power source to light two hundreds of light-emitting diodes (LEDs) connected in antiparallel and is also used to charge a 110 μF commercial capacitor to 6.0 V in 23 s. Due to the spiral-like electrode structure, the electromagnetic induced electricity can also be generated by sticking a small magnet on the rotating disk, which is different from the other hybrid generators that two independent electrode systems must be needed. The electromagnetic induced short-circuit current, open-circuit voltage, and maximum power of the generator are measured. This work presents a novel electrode structure which demonstrates the double functions of the spiral-like electrodes for triboelectricity and electromagnetic induced electricity. It indicates that the electrode design is important for the realization of multifunction and application in some special situations for electronic device integration.

2. EXPERIMENTAL SECTION

2.1. Fabrication of Single PSE Generator. *(I). Fabrication of Immobile Electrode Part.*

(1) A piece of commercial aluminum foil with width, length, and thickness of 150 mm, 150 mm, and 100 μm was pasted on a polyethylene terephthalate (PET) film with width, length, and thickness of 150 mm, 150 mm, and 0.065 mm, respectively.
(2) The aluminum foil was cut into the designed spiral-like electrode strips in two for electrode-1 and electrode-2 with 1, 2, and 3 cycles for G1#, G2#, and G3# generators respectively by a laser cutter (SDM50). These three generators have the same working period as is shown in Video 1.
(3) The spiral-like aluminum foil electrodes were stuck to a transparent acrylic disk (diameter: 100 mm) and the PET film was turned to the upper surface with a sandwiched structure of acrylic disk/electrodes/PET. The two spiral-like Al strips connected through the external circuit acting as the electrodes of the TENG part, while two Cu wires were connected to the both ends of a single spiral-like Al strip as the electrodes of the EMG part.

(II). Fabrication of the Rotational Part. The spiral-like PTFE strip with 1, 2, and 3 cycles was cut to match the electrode strip and then was stuck to another acrylic disk with diameter of 95 mm, which was fixed on a rotation axes driven by an electrical motor. Besides, a permanent magnet with radius of 20 mm and height of 5 mm was fixed on the margin of the disk.

2.2. Fabrication of an Integrated PSE-Triboelectric Generator. The multilayered PSE-triboelectric generator is mainly composed of two groups: rotors and stators. The electrode disk was covered by spiral-like electrodes on both sides with the structure of PET/electrodes/acrylic disk/electrodes/PET. The PTFE disk was covered by PTFE strips on both sides with structure of PTFE/acrylic disk/PTFE. Four electrode disks with bigger holes in the center were set as stators and three PTFE disks with smaller holes in the center were set as rotors, which are fixed on a rotation axes by matching the size of the holes in the center. The diameter of stators is larger than that of rotators so as to fix them easily. Then the integrated PSE-triboelectric generator was obtained by stacking four stators and three rotors in an alternating sequence with the axes going through the center-holes of them.

2.3. Characterization of PSE-Triboelectric Generator. The output performance of PSE-triboelectric generator was measured using a Stanford low-noise current preamplifier (model SR570) and a Data Acquisition Card (NI PCI-6259). In this measurement, the electrode part was fixed on a stationary support, and an electrical motor (51K40RA-D1500) with a digital display speed controller was employed to produce a rotating motion with different speeds on the movable PTFE part.

3. RESULTS AND DISCUSSION

As is shown in Figure 1a, the basic structure of the PSE-triboelectric generator consists of the free-standing rotational

DOI: 10.1021/acsami.5b03613
ACS Appl. Mater. Interfaces 2015, 7, 16450−16457

part of tribocharged layer and the immobile part of metal electrodes. The immobile disk of metal electrodes has two spiral-like electrode strips (Figure 1a1) and the rotational disk of tribocharged layer has one PTFE spiral-like strip (Figure 1a2). Figure 1a3 displays the whole structure of the PSE-triboelectric generator. A digital photograph of the PSE-triboelectric generator is shown in Figure 1b, which illustrates two spiral-like electrodes and one PTFE spiral-like strip on two acrylic disks, respectively. In order to study the influence of the electrode structure on output current, three PSE-triboelectric generators have been fabricated, which consist of different cycles of the spiral-like electrodes and the PTFE spiral-like strip named as G1#, G2# and G3#, respectively, as is shown in Figure 1c.

The working mechanism of the PSE-triboelectric generator is illustrated in Figure 2a–e. Although the structure is different from the sliding TENGs previously reported,[31] the working principle is similar. When the PTFE disk turns a circle, the transfer of electrons between the electrodes will complete one cycle. Figure 2a shows the initial state in one cycle, where the aluminum electrode-1 is fully overlapped by the PTFE sandwiched with the PET film. The electrons will be injected from PET to the PTFE film leaving negative charges on the PTFE film and positive charges on the PET film due to the triboelectric effect. Meanwhile, positive and negative charges appear on the electrode-1 and electrode-2, respectively, by the electrostatic induction. When the PTFE strip moves from the state of fully overlapped electrode-1 to the state of overlapped electrode-2, the electrons transfer from electrode-2 to electrode-1 by the induced potential difference across the two electrodes, producing a current flowing from electrode-1 to electrode-2 through the external circuit, as is shown in Figure 2b. The charge transfer will continue until it reaches the state in Figure 2c. Then the PTFE strip will inversely move from electrode-2 to electrode-1. Similarly, the electrons will drive from electrode-1 to electrode-2, resulting in an output current from electrode-2 to electrode-1 (Figure 2d) until the PTFE strip fully overlaps the electrode-1 (Figure 2e). Thus, a complete cycle of electricity generation has been accomplished.

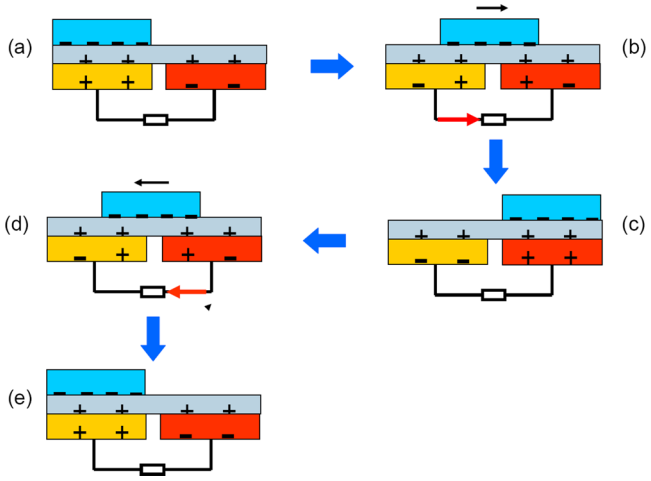

Figure 2. Schematic illustrations of the charge distributions and electricity generation process when the PSE-triboelectric nanogenerator rotates a full cyclic (a–e).

To study the cycle number of the spiral-like strip and rotating speed, the output performance of three PSE-triboelectric generators (G1#, G2#, and G3#) is measured at different rotating speeds, as is shown in Figure 3. The rotating speed can be controlled by an electrical motor with a digital display speed controller. In order to keep the PSE-triboelectric generators immovable, the electrode disks are fixed on a stationary support in the experiment. Figure 3a1–3 exhibit a short-circuit current, the open circuit voltage, and the transferred charge density in half a cycle of the G1# at rotating speed of 100, 200, 300, 400, and 500 r/min, respectively. As is shown in Figure 3a1–2, the output current of the G1# increases with an increase in the rotating speed, and the maximum output current reaches to 6.2 μA at a rotating speed of 500 r/min. The V_{oc} in this work is

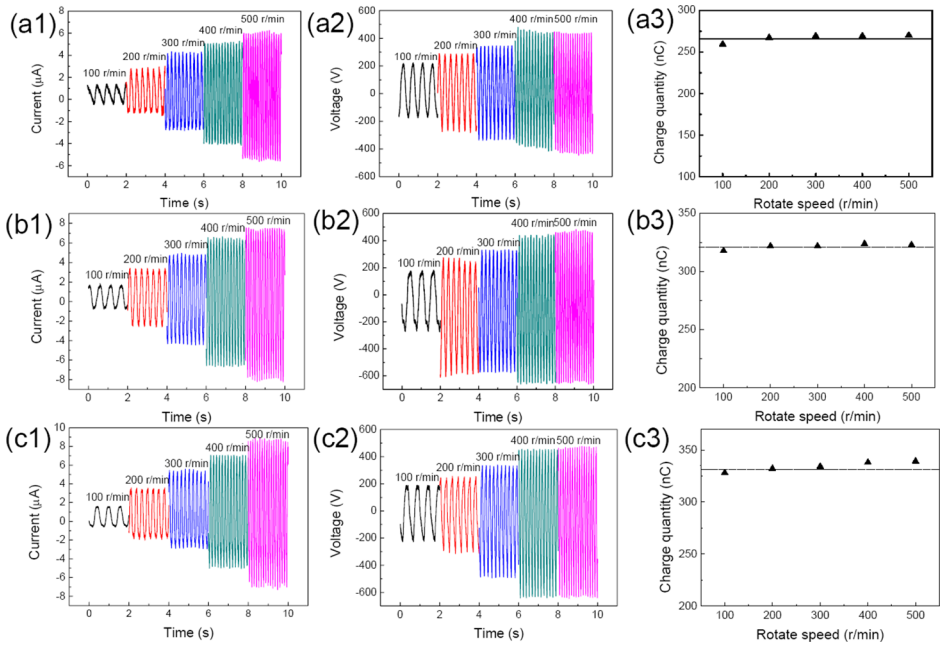

Figure 3. Output of the PSE-triboelectric nanogenerator with the thin PET film (0.065 mm). The output short current, open-circuit voltage and charge transfer in half cycle of G1# (a), G2# (b), and G3#(c) with different rotating speeds from 100 to 500 r/min.

DOI: 10.1021/acsami.5b03613
ACS Appl. Mater. Interfaces 2015, 7, 16450–16457

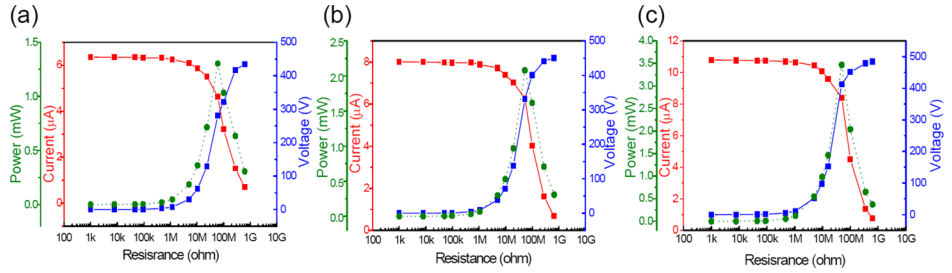

Figure 4. Output current, voltage and the power for the G1# (a), G2# (b), and G3# (c) with the thin PET film (0.065 mm) versus different external resistances at rotating speed of 700 r/min.

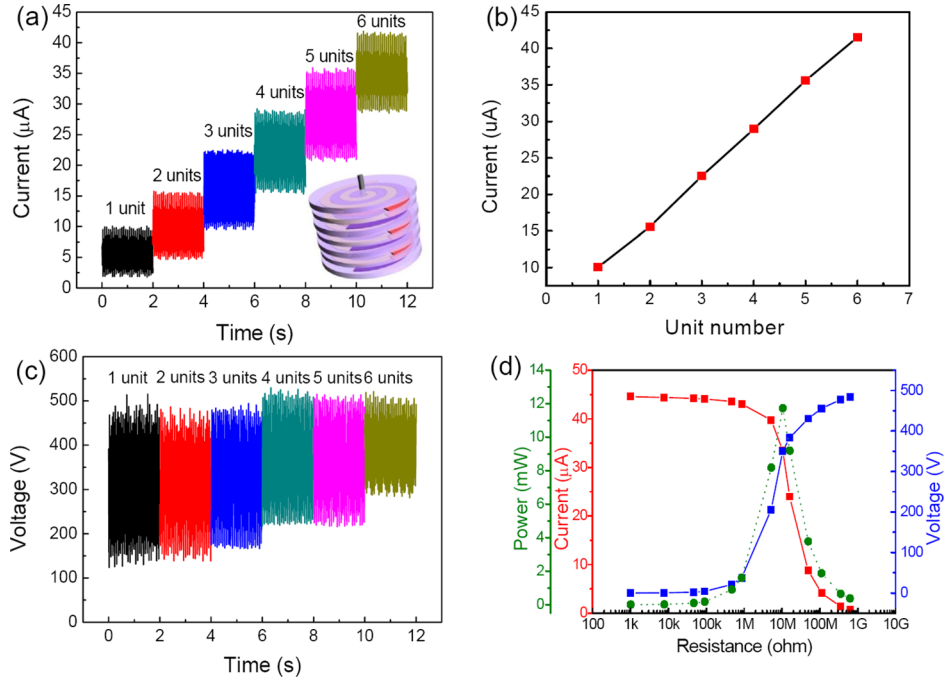

Figure 5. Short current (a, b) and open-circuit voltage (c) of the multilayered PSE-triboelectric nanogenerator with one, two, three, four, five and six of G2# unit. The plots of the short current, open-circuit voltage and output power of the multilayered PSE-triboelectric nanogenerator with six G2# units (d). The inset shows the schematic structure of the multilayered PSE-triboelectric nanogenerator.

measured under the external load resistance of 100 MΩ. The output voltage increases with an increase in rotating speed from 100 to 400 r/min and tends to be a constant after the rotating speed reaches to 400 r/min. The charge transfer quantity of the G1# in half a cycle at the different rotating speeds is a constant of about 270 nC, as is shown in Figure 3a3. Compared with the G1#, the output current and voltage of the G2# and G3# have similar change versus rotating speed (Figure 3b1−b2 and c1−c2). Figure 3a1−c1 and a2−c2 reveal clearly that the magnitude of the output current and voltage for these three generators are in the sequence G3# > G2# > G1# at the same rotating speed, which demonstrates the output current and output voltage increase with the cycle number of the spiral-like strip. The maximum output current and voltage for the G3# are 9.0 μA and 470 V, respectively. The charge transfer quantity for the G2# and G3# is 320 nC and 330 nC, respectively (Figure 3b3,c3). The output current of triboelectric generator with different numbers of cycle of the spiral-like electrode and at different rotating speeds are shown in Figure S1 a1. By increasing the cycle number of the spiral-like electrode at the same rotating speeds (100−500 r/min), the output current can be enhanced at the fixed rotating speed respectively as is shown in Figure S1 a2. As we all know, the capacitance (C) of the triboelectric generator is related to the structure of electrodes, including electrode area (S) and the gap between the two spiral-like electrodes (d). Since the S becomes larger with an increase in the cycle number of the spiral-like electrode and the d has little change, the C will increase. On the other hand, as the capacitance is determined by eq 1

$$C = \frac{Q_{elel}}{V} = \frac{\Delta\sigma_{elel} S}{V_{oc}} \quad (1)$$

where $\Delta\sigma_{elel}$ is the density of the transferred charge on one electrode in a half period and the V_{OC} is related to the area of the electrode S

$$V_{oc} = \frac{\Delta\sigma_{SC} S}{C} \quad (2)$$

which increases with the increase in the cycle number of the spiral electrode. According to the Ohm law, the current is proportional to the output voltage at a constant of the internal resistance of the generator, and the output current is also affected by the cycle number of the spiral electrode.

The influence of thickness of PET film sandwiched between electrode disk and PTFE disk has been investigated by

DOI: 10.1021/acsami.5b03613
ACS Appl. Mater. Interfaces 2015, 7, 16450−16457

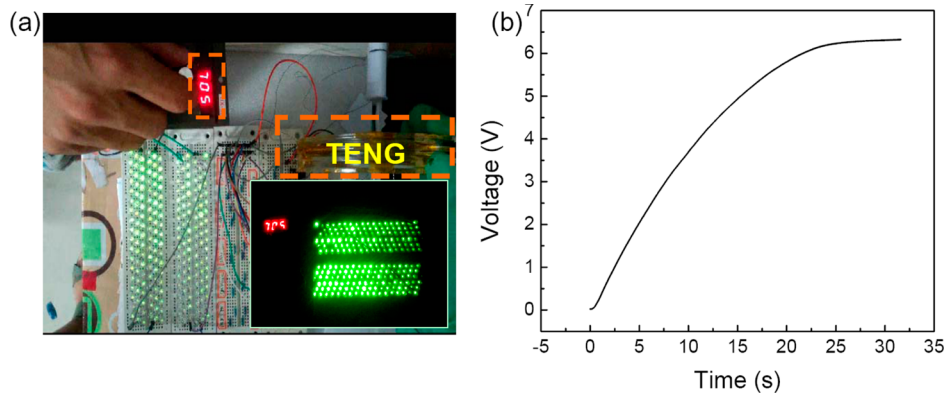

Figure 6. (a) Digital photographs of the multilayered PSE-triboelectric nanogenerator light up 200 LEDs connected in antiparallel. (b) The time-voltage curve in the charging process for a 110 μF commercial capacitor.

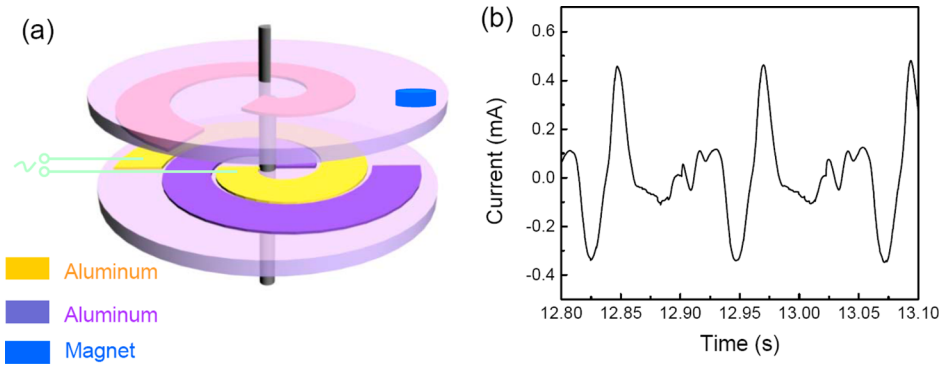

Figure 7. (a) Device structure of the PSE-electromagnetic generator. (b) Enlarged view of the current curves.

changing the thickness from 0.065 mm to 0.09 mm for the G1#-G3# and the results are shown in Figure S2 and Table S1, from which we can see that the PET thickness does not affect the change trend of output performance of these triboelectric generators under different rotating speeds, but decreases the outputs by increasing the thickness. As the induced charges decrease with an increase in the vertical distance between PTEF and Al electrodes, the output performance with thinner PET film can be enhanced.[33]

The output performance of the PSE-triboelectric generators versus the external load is shown in Figure 4. Normally, the output current decreases with an increase in load resistance, while the output voltage displays an opposite trend. In this experiment, all the PSE-triboelectric generators work at the rotating speed of 700 r/min. As are exhibited in Figure 4a–c, the maximum output voltage and current of the G1#, G2#, and G3# are 434 V and 6.35 μA, 450 V and 8.0 μA, and 475 V and 10.8 μA, respectively, indicating that the output performance of these PSE-triboelectric generators increases with the cycle number of the spiral-like strip. The maximum output power of the G1#, G2#, and G3# is 1.3, 2.08, and 3.46 mW under the external load resistance of 50 MΩ.

To further improve the output power, we make an integrated PSE-triboelectric generator as is shown in the inset of Figure 5a. The rectified current of the integrated PSE-triboelectric generator with different numbers of G2# unit at the rotating speed of 700 r/min is shown in Figure 5a, from which we can observe that the short-circuit current increases from 10.05 to 41.55 μA with the number of G2# unit from one to six. Figure 5b exhibits that the short-circuit current increases linearly with the number of single G2# unit. The open-circuit voltage of the integrated PSE-triboelectric generator is almost maintained at 500 V, which is independent of the number of G2# unit due to the fact that integrated G2# units are connected in parallel (Figure 5c). In addition, the peak output power, current and voltage as a function of load resistance for the integrated PSE-triboelectric generator is also measured. Figure 5d shows the maximum output power is 11.73 mW under the load resistance of 10 MΩ.

The integrated PSE-triboelectric generator can be applied to light 200 LEDs connected in antiparallel due to its high output power, as is shown in Figure 6a and Video 2 (Supporting Information). As a power supply, an electronic device often needs a constant current and relatively low bias, the high output voltage and alternating pulse current cannot directly be utilized to power it in most cases. To obtain a stable the output power, we store the output power in a commercial capacitor (110 μF). The charging voltage–time plot is shown in Figure 6b, from which we can see that the capacitor is charged to 6 V within 23 s by the intergraded PSE-triboelectric generator.

To exhibit the extraordinary advantages of the novel planar spiral-like electrodes compared with fan shape electrodes, a permanent magnet is fixed on the edge of the acrylic disk to harvest rotation energy by electromagnetic induced electricity in the same time as is shown in Figure 7a. Two Cu wires are connected to the ends of a single spiral-like Al strip to collect the output current. The spiral electrode structure can be used as coils to collect electromagnetic inducted electricity, which is quite different from the other hybrid generators that they employ additional Cu coils to collect electromagnetic induced electricity.

DOI: 10.1021/acsami.5b03613
ACS Appl. Mater. Interfaces 2015, 7, 16450–16457

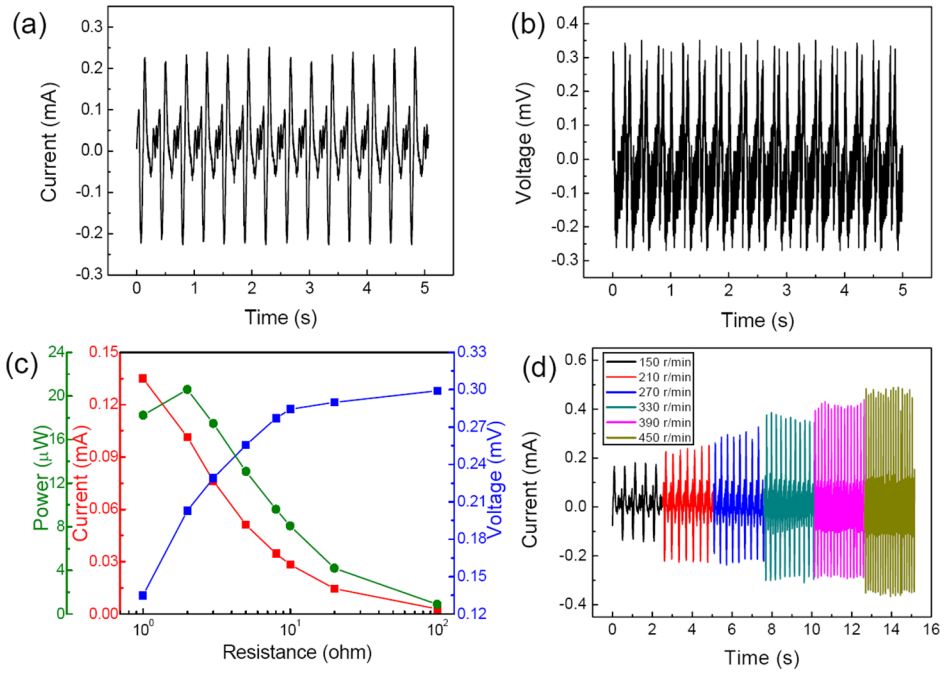

Figure 8. Output performance of the PSE-electromagnetic generator. The short current (a) and the open-circuit voltage (b) at a rotating speed of 200 r/min. The output current, the voltage, and the power with different external resistance (c). The output short current with different rotating speeds from 150 to 450 r/min (d).

As we all know, for the electromagnetic induction, the induced electromotive force is determined by

$$E = n\frac{d\phi}{dt} = n\cdot\left(\vec{B}\frac{d\vec{S}}{dt} + \vec{S}\frac{d\vec{B}}{dt}\right) \quad (3)$$

where n is the number of windings, and $d\phi/dt$ is the change rate of magnetic flux in each winding. B is the magnetic flux density, and S is the area circled by winding.[34] For the PSE-electromagnetic generator, the winding is a single spiral-like electrode strip (coil) and S is the area circled by a coil, which is a constant. Thus, the electricity generation is related to the change rate of magnetic flux density. When the acrylic disk begins rotating, the spatial distribution of the magnetic field introduced by the magnet fixed on the disk is changed. Therefore, the magnetic flux in the coil is altered and leads to the generation of an electromagnetic induction current. When the PSE-electromagnetic generator rotates a cycle, a current pulse is generated as depicted in Figure 7b.

Figure 8 shows the output performance of the PSE-electromagnetic generator with one cycle of the spiral-like electrode strip when it works independently. The corresponding I_{sc} and V_{oc} are about 0.25 mA and 0.32 mV at a rotating rate of 200 r/min in Figure 8a,b, respectively. As is depicted in Figure 8c, the output current of the PSE-electromagnetic generator decreases with an increase in the loading resistance, but the voltage increases, and the maximum output power is about 20.64 μW at the loading resistance of 2 Ω. The short-circuit current also increases linearly with an increase in the rotating speed as the change rate of magnetic flux increases accordingly, as is shown in Figure 8d. At a rotating speed of 450 r/min, the short-circuit current for the PSE-electromagnetic generator reaches 0.47 mA.

According to the results in Figures 4 and 8c, the generator working in triboelectric mode with high internal resistance (50 MΩ) can be used as a current source, while the generator working in electromagnetic mode with low internal resistance (2 Ω) can be used as a voltage source, respectively.

In order to further find out whether there is interference between the triboelectric and electromagnetic modes, a comparison is given in Figure S4. The output current of the PSE-generator working in the triboelectric mode without a magnet is about 5.8 μA, which is almost the same as that with the sticking of a magnet. It demonstrates that the output of triboelectricity is not affected by the electromagnetic inducted electricity. Moreover, the output performance of the two mode generators connected in series and parallel were measured. The output current of the two mode generators connected in series is the same as the PSE-generator working in triboelectric mode due to its high resistance (current source). On the other hand, the two mode generators cannot be connected in parallel which will result in a short circuit.

4. CONCLUSIONS

In summary, we have demonstrated a novel planar spiral-like electrode structure that is capable of effectively harvesting the rotational mechanical energy. The PSE-generator can work simultaneously in triboelectricity and electromagnetic induced electricity modes due to the spiral-like electrode structure. The maximum open-circuit voltage and short-circuit current are 470 V and 9.0 μA at rotating speed of 500 r/min for the PSE-triboelectric generator with three cycles of the spiral-like electrode strip. The coaxially integrated multilayered spiral-like PSE-triboelectric generator can enhance the output of the power effectively. The short-circuit current, an open-circuit voltage, and the output power reach 41.55 μA, 500 V, and 11.73 mW, respectively, at a rotating speed of 700 r/min by the six layer electrode (two cycles) integration. The output power of the multilayered PSE-triboelectric generator can drive 200 LEDs connected in antiparallel or charge a 110 μF commercial capacitor to 6 V in 23 s. Meanwhile, for the PSE-electro-

DOI: 10.1021/acsami.5b03613
ACS Appl. Mater. Interfaces 2015, 7, 16450−16457

magnetic generator, the maximum current, voltage, and power in a single electrode strip are about 0.25 mA, 0.32 mV, and 20.64 μW, respectively. This work presents a novel electrode structure which demonstrates dual function of the spiral-like electrodes for triboelectricity and electromagnetic induced electricity.

■ ASSOCIATED CONTENT

Supporting Information

Figures S1−S5 and videos 1 and 2 as mentioned in the text. The Supporting Information is available free of charge on the ACS Publications website at DOI: 10.1021/acsami.5b03613.

■ AUTHOR INFORMATION

Corresponding Author

*Tel: +86 23 65678362. Fax: +86 23 65678362. E-mail: hucg@cqu.edu.cn.

Notes

The authors declare no competing financial interest.

■ ACKNOWLEDGMENTS

This work is supported by the National High Technology Research and Development Program of China (2015AA034801), Chongqing University Phostgraduates' Innovation Project (CYB15044), NSFC (11204388), the Fundamental Research Funds for the Central Universities (CQDXWL-2014-001 and CQDXWL-2013-012), and the large-scale equipment sharing fund of Chongqing University.

■ REFERENCES

(1) Wang, Z. L.; Zhu, G.; Yang, Y.; Wang, S. H.; Pan, C. F. Progress in Nanogenerators for Portable Electronics. *Mater. Today* **2012**, *15*, 532−543.

(2) Mitcheson, P. D.; Yeatman, E. M.; Rao, G. K.; Holmes, A. S.; Green, T. C. Energy Harvesting from Human and Machine Motion for Wireless Electronic Devices. *Proc. IEEE* **2008**, *96*, 1457−1486.

(3) Zhu, G.; Pan, C.; Guo, W.; Chen, C. Y.; Zhou, Y.; Yu, R.; Wang, Z. L. Triboelectric-Generator-Driven Pulse Electrodeposition for Micropatterning. *Nano Lett.* **2012**, *12*, 4960−4965.

(4) Zhong, J.; Zhong, Q.; Fan, F.; Zhang, Y.; Wang, S.; Hu, B.; Wang, Z. L.; Zhou, J. Finger Typing Driven Triboelectric Nanogenerator and Its Use for Instantaneously Lighting Up LEDs. *Nano Energy* **2013**, *2*, 491−497.

(5) Wang, S.; Lin, L.; Xie, Y.; Jing, Q.; Niu, S.; Wang, Z. L. Sliding-Triboelectric Nanogenerators Based on In-Plane Charge-Separation Mechanism. *Nano Lett.* **2013**, *13*, 2226−2233.

(6) Zhang, Z.; Liao, Q. L.; Yan, X. Q.; Wang, Z. L.; Wang, W. D.; Sun, X.; Lin, P.; Huang, Y. H.; Zhang, Y. Functional Nanogenerators as Vibration Sensors Enhanced by Piezotronic Effects. *Nano Res.* **2014**, *7*, 190−198.

(7) Zhang, X. H.; Fang, J. L.; Meng, F. F.; Wei, X. L. A Novel Self-Powered Wireless Sensor Node Based on Energy Harvesting for Mechanical Vibration Monitoring. *Math. Probl. Eng.* **2014**, *2014*, 642365.

(8) Wang, Z. L.; Song, J. H. Piezoelectric Nanogenerators Based on Zinc Oxide Nanowire Arrays. *Science* **2006**, *312*, 242−246.

(9) Wang, X. D.; Song, J. H.; Liu, J.; Wang, Z. L. Direct-Current Nanogenerator Driven by Ultrasonic Waves. *Science* **2007**, *316*, 102−105.

(10) Qin, Y.; Wang, X. D.; Wang, Z. L. Microfibre−Nanowire Hybrid Structure for Energy Scavenging. *Nature* **2008**, *451*, 809−813.

(11) Chang, C.; Tran, V. H.; Wang, J. B.; Fuh, Y. K.; Lin, L. W. Direct-Write Piezoelectric Polymeric Nanogenerator with High Energy Conversion Efficiency. *Nano Lett.* **2010**, *10*, 726−731.

(12) Lee, J. H.; Lee, K. Y.; Gupta, M. K.; Kim, T. Y.; Lee, D. Y.; Oh, J.; Ryu, C. K.; Yoo, W. J.; Kang, C. Y.; Yoon, S. J.; Yoo, J. B.; Kim, S. W. Highly Stretchable Piezoelectric-Pyroelectric Hybrid Nanogenerator. *Adv. Mater.* **2014**, *26*, 765−769.

(13) Fan, F.-R.; Tian, Z.-Q.; Wang, Z. L. Flexible Triboelectric Generator. *Nano Energy* **2012**, *1*, 328−334.

(14) Liu, G. L.; Leng, Q.; Lian, J. W.; Guo, H. Y.; Yi, Y.; Hu, C. G. Notepad-Like Triboelectric Generator for Efficiently Harvesting Low-Velocity Motion Energy by Interconversion between Kinetic Energy and Elastic Potential Energy. *ACS Appl. Mater. Interfaces* **2015**, *7*, 1275−1283.

(15) Wang, S. H.; Lin, L.; Wang, Z. L. Nanoscale Triboelectric-Effect-Enabled Energy Conversion for Sustainably Powering Portable Electronics. *Nano Lett.* **2012**, *12*, 6339−6346.

(16) Lee, S.; Bae, S. H.; Lin, L.; Yang, Y.; Park, C.; Kim, S. W.; Cha, S. N.; Kim, H. J.; Park, Y. J.; Wang, Z. L. Super-Flexible Nanogenerator for Energy Harvesting from Gentle Wind and as an Active Deformation Sensor. *Adv. Funct. Mater.* **2013**, *23*, 2445−2449.

(17) Yang, Y.; Guo, W. X.; Pradel, K. C.; Zhu, G.; Zhou, Y. S.; Zhang, Y.; Hu, Y. F.; Lin, L.; Wang, Z. L. Pyroelectric Nanogenerators for Harvesting Thermoelectric Energy. *Nano Lett.* **2012**, *12*, 2833−2838.

(18) Yang, Y.; Wang, S.; Zhang, Y.; Wang, Z. L. Pyroelectric Nanogenerators for Driving Wireless Sensors. *Nano Lett.* **2012**, *12*, 6408−6413.

(19) Leng, Q.; Chen, L.; Guo, H. Y.; Liu, J. L.; Liu, G. L.; Hu, C. G.; Xi, Y. Harvesting Heat Energy from Hot/Cold Water with a Pyroelectric Generator. *J. Mater. Chem. A* **2014**, *2*, 11940−11947.

(20) Xie, Y. N.; Wang, S. H.; Lin, L.; Jing, Q. S.; Lin, Z. H.; Lin, S. M.; Wu, Z. Y.; Wang, Z. L. Rotary Triboelectric Nanogenerator Based on a Hybridized Mechanism for Harvesting Wind Energy. *ACS Nano* **2013**, *7*, 7119−7125.

(21) Hu, Y. F.; Yang, J.; Jing, Q. S.; Niu, S. M.; Wu, W. Z.; Wang, Z. L. Triboelectric Nanogenerator Built on Suspended 3D Spiral Structure as Vibration and Positioning Sensor and Wave Energy Harvester. *ACS Nano* **2013**, *7*, 10424−10432.

(22) Hou, T. C.; Yang, Y.; Zhang, H. L.; Chen, J.; Chen, L. J.; Wang, Z. L. Triboelectric Nanogenerator Built Inside Shoe Insole for Harvesting Walking Energy. *Nano Energy* **2013**, *2*, 856−862.

(23) Hu, Y. F.; Yang, J.; Niu, S. M.; Wu, W. Z.; Wang, Z. L. Hybridizing Triboelectrification and Electromagnetic Induction Effects. *ACS Nano* **2014**, *8*, 7442−7450.

(24) Bai, P.; Zhu, G.; Lin, Z.-H.; Jing, Q.; Chen, J.; Zhang, G.; Ma, J.; Wang, Z. L. Integrated Multilayered Triboelectric Nanogenerator for Harvesting Biomechanical Energy from Human Motions. *ACS Nano* **2013**, *7*, 3713−3719.

(25) Yang, X.; Zhu, G.; Wang, S.; Zhang, R.; Lin, L.; Wu, W.; Wang, Z. L. A Self-Powered Electrochromic Device Driven by a Nanogenerator. *Energy Environ. Sci.* **2012**, *5*, 9462−9466.

(26) Lin, Z.-H.; Zhu, G.; Zhou, Y.; Yang, Y.; Bai, P.; Chen, J.; Wang, Z. L. A Self-Powered Triboelectric Nanosensor for Mercury Ion Detection. *Angew. Chem., Int. Ed.* **2013**, *19*, 5065−5069.

(27) Yang, Y.; Lin, L.; Zhang, Y.; Jing, Q.; Hou, T. C.; Wang, Z. L. Self-Powered Magnetic Sensor Based on a Triboelectric Nanogenerator. *ACS Nano* **2012**, *6*, 10378−10383.

(28) Arnold, D. P. Review of Microscale Magnetic Power Generation. *IEEE Trans. Magn.* **2007**, *43*, 3940.

(29) Lin, L.; Wang, S. H.; Niu, S. M.; Liu, C.; Xie, Y. N.; Wang, Z. L. Noncontact Free-Rotating Disk Triboelectric Nanogenerator as a Sustainable Energy Harvester and Self-Powered Mechanical Sensor. *ACS Appl. Mater. Interfaces* **2014**, *6*, 3031−3038.

(30) Zhou, T.; Zhang, C.; Han, C. B.; Fan, F. R.; Tang, W.; Wang, Z. L. Woven Structured Triboelectric Nanogenerator for Wearable Devices. *ACS Appl. Mater. Interfaces* **2014**, *6*, 14695−14701.

(31) Guo, H. Y.; Leng, Q.; He, X. X.; Wang, M. J.; Chen, J.; Hu, C. G.; Xi, Y. Triboelectric Generator Based on Checker-Like Interdigital Electrodes with a Sandwiched PET Thin Film for Harvesting All Direction Sliding Energy. *Adv. Energy Mater.* **2015**, *5*, 1400790.

(32) Guo, H. Y.; Chen, J.; Leng, Q.; Xi, Y.; Wang, M. J.; He, X. X.; Hu, C. G. Spiral-Interdigital-Electrode-Based Multifunctional Device:

DOI: 10.1021/acsami.5b03613
ACS Appl. Mater. Interfaces 2015, 7, 16450−16457

Dual-Functional Triboele-ctric Generator and Dual-Functional Self-Powered Sensor. *Nano Energy* **2015**, *12*, 626−635.
(33) Leng, Q.; Guo, H. Y.; He, X. X.; Liu, G. L.; Kang, Y.; Hu, C. G.; Xi, Y. Flexible interdigital-electrodes-based triboelectric generators for harvesting sliding and rotating mechanical energy. *J. Mater. Chem. A* **2014**, *2*, 19427−19434.
(34) Zhang, C.; Tang, W.; Han, C. B.; Fan, F. R.; Wang, Z. L. Theoretical Comparison, Equivalent Transformation, and Conjunction Operations of Electromagnetic Induction Generator and Triboelectric Nanogenerator for Harvesting Mechanical Energy. *Adv. Mater.* **2014**, *26*, 3580−3591.

DOI: 10.1021/acsami.5b03613
ACS Appl. Mater. Interfaces 2015, 7, 16450−16457